

## Electronic Supplementary Information (ESI)

# Ag<sup>+</sup> Coordination Polymers of a Chiral Thiol Ligand Bearing an AIE Fluorophore

*Dan-Dan Tao, Qian Wang, Xiao-Sheng Yan, Na Chen, Zhao Li and Yun-Bao Jiang\**

*Department of Chemistry, College of Chemistry and Chemical Engineering, the MOE Key  
Laboratory of Spectrochemical Analysis and Instrumentation, and the Collaborative  
Innovation Centre of Chemistry for Energy Materials (iChEM), Xiamen University,  
Xiamen 361005, China*

E-mail: [ybjiang@xmu.edu.cn](mailto:ybjiang@xmu.edu.cn)

## TABLE OF CONTENTS

<b>S1. Experimental.....</b>	<b>2</b>
<b>S1.1 General.....</b>	<b>2</b>
<b>S1.2 Synthesis.....</b>	<b>2</b>
<b>S1.3 References.....</b>	<b>3</b>
<b>S2. Additional Data.....</b>	<b>4</b>
<b>S2.1 Spectral data.....</b>	<b>4</b>
<b>S2.2 <sup>1</sup>H and <sup>13</sup>C NMR spectra.....</b>	<b>16</b>

## S1. EXPERIMENTAL

### S1.1 GENERAL

All chemicals and solvents purchased from Energy Chemical, except otherwise described, were used without further purification. THF used in anhydrous syntheses was further refluxed over metallic sodium in the presence of benzophenone until a persistent blue color was obtained and then it was distilled under nitrogen. <sup>1</sup>H NMR and <sup>13</sup>C NMR spectra were recorded using Ascend III-500 in CDCl<sub>3</sub> with TMS. Absorption spectra were recorded on a Thermo Evolution 300 spectrophotometer. CD spectrometry was conducted using JASCO J-810 Circular Dichroism Chiroptical Spectrometer. Steady state fluorescence measurements were conducted using a HITACHI F-4500 spectrofluorometer. HRMS (high-resolution MS) was recorded on Bruker Impact II. 4-(1,2,2-Triphenylvinyl)benzoic acid (TPE-CO<sub>2</sub>H) **5** was prepared according to literature procedures.

### S1.2 SYNTHESIS

**TPECOOH, 5**: The compound was synthesized according to the synthetic route shown in Scheme S1. Typical procedures for its synthesis are shown as follows. To a solution of diphenylmethane, **2** (2.02 g, 12 mmol) in dry tetrahydrofuran (50 mL) was added 6.25 mL of a 1.6 M solution of *n*-butyllithium in hexane (10 mmol) at -78 °C under a nitrogen atmosphere. The resulting orange-red solution was stirred for 30 min at that temperature, to this solution was added 4-bromobenzophenone, **3** (2.35 g; 9 mmol). Afterwards, the reaction mixture was allowed to warm to room temperature and stirred for another 6 h. The reaction was quenched with the addition of an aqueous solution of ammonium chloride. The organic layer was then extracted with dichloromethane (3 × 50 mL). The organic layers were combined, washed with saturated brine solution and dried over anhydrous magnesium sulphate. After solvent evaporation, the resulting crude alcohol (containing excess diphenylmethane) was subjected to acid-catalyzed dehydration without further purification. The crude alcohol was dissolved in about 80 mL of toluene in a 100 mL Schlenk flask fitted with a Dean-Stark trap. A catalytic amount of *p*-toluenesulfonic acid (342 mg; 1.8 mmol) was added and the mixture was refluxed for 3-4 h. After the reaction mixture was cooled to room temperature, the toluene layer was washed with 10% aqueous NaHCO<sub>3</sub> solution (2 × 25 mL) and dried over anhydrous magnesium sulfate. Evaporation of the solvent under reduced pressure afforded the crude tetraphenylethene derivative, which was further purified by silica gel column chromatography using hexane as eluent, **4**. To a solution of **4** (1.6 g; 3.89 mmol) in 30 mL dry THF was added dropwise 2.9 mL (4.64 mmol) of *n*-butyllithium (1.6 M in *n*-hexane) at -78 °C under stirring. The reaction mixture was stirred for 2 h to get a dark brown solution. To the obtained solution was then added dry ice pieces in small portions under nitrogen. The solution was allowed to warm to room temperature and stir for additional 12 h. The solvent was evaporated

under reduced pressure. The crude product was purified on a silica-gel column using dichloromethane/methanol mixture (90/10 v/v) as eluent **5** (0.9 g, 62% yield).

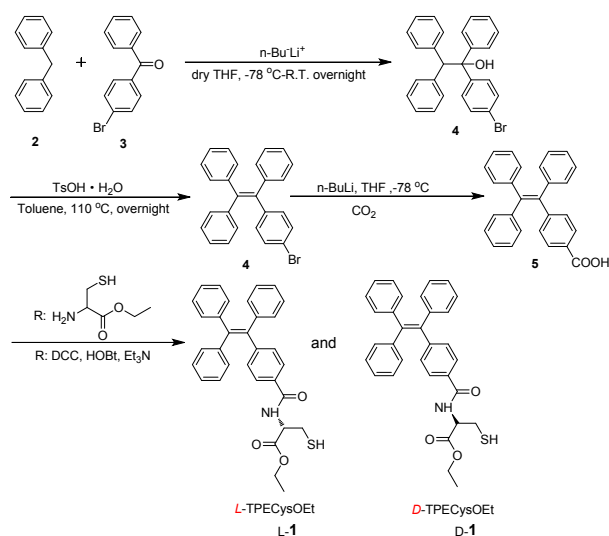
**TPECysOEt, 1:** To a solution of L/D-cysteine ethyl ester (2 mmol), 1-hydroxybenzotriazole (2 mmol) and triethylamine (2 mmol) in CH<sub>2</sub>Cl<sub>2</sub> (10 mL) was added the corresponding **5** (2 mmol). The mixture was stirred at 0 °C for 20 min, and then dicyclohexylcarbodiimide (2 mmol) was added and stirred at room temperature for 4 h. After filtration and solvent evaporation, the crude product was purified by silica gel column chromatography and light yellow powder of L/D-**1** was obtained (0.5 g, 67% yield).

**PhCysOEt, L-2:** To a solution of L/D-cysteine ethyl ester (2 mmol), 1-hydroxybenzotriazole (2 mmol) and triethylamine (2 mmol) in CH<sub>2</sub>Cl<sub>2</sub> (10 mL) was added the corresponding benzoic acid (2 mmol). The mixture was stirred at 0 °C for 20 min, and then dicyclohexylcarbodiimide (2 mmol) was added and stirred at room temperature for 4 h. After filtration and solvent evaporation, the crude product was purified by silica gel column chromatography and light yellow powder of L/D-**1** was obtained (56% yield).

**D-1:** <sup>1</sup>H NMR (500 MHz, CDCl<sub>3</sub>) δ/ppm 8.89 (d, *J* = 7.7 Hz, 1H), 7.67 (d, *J* = 8.3 Hz, 1H), 7.60 (d, *J* = 8.2 Hz, 1H), 7.08 (m, 17H), 4.55 (dd, *J* = 13.6, 8.2 Hz, 1H), 4.12 (dd, *J* = 14.0, 6.9 Hz, 2H), 3.63 (dd, *J* = 13.6, 4.9 Hz, 2H), 1.28 (d, *J* = 11.9 Hz, 1H), 1.24 (m, 3H); <sup>13</sup>C NMR (126 MHz, CDCl<sub>3</sub>) δ/ppm 170.19, 166.77, 147.92, 143.23, 143.11, 142.32, 139.73, 131.59, 131.25, 131.22, 131.14, 127.90, 127.81, 127.68, 126.87, 126.70, 126.59, 62.16, 53.88, 26.99, 14.22; HRMS (ESI): calcd for [C<sub>32</sub>H<sub>29</sub>NO<sub>3</sub>S]<sup>-</sup>: 506.1784, found: 506.1729.

**L-1:** <sup>1</sup>H NMR (500 MHz, CDCl<sub>3</sub>) δ/ppm 8.89 (d, *J* = 7.7 Hz, 1H), 7.67 (d, *J* = 8.3 Hz, 1H), 7.60 (d, *J* = 8.2 Hz, 1H), 7.08 (m, 17H), 4.55 (dd, *J* = 13.6, 8.2 Hz, 1H), 4.12 (dd, *J* = 14.0, 6.9 Hz, 2H), 3.63 (dd, *J* = 13.6, 4.9 Hz, 2H), 1.28 (d, *J* = 11.9 Hz, 1H), 1.24 (m, 3H); <sup>13</sup>C NMR (126 MHz, CDCl<sub>3</sub>) δ/ppm 170.19, 166.73, 147.89, 143.23, 143.10, 142.31, 139.73, 131.58, 131.25, 131.24, 131.21, 131.16, 127.90, 127.80, 127.67, 126.86, 126.69, 126.58, 62.14, 53.87, 26.98, 14.21; HRMS (ESI): calcd for [C<sub>32</sub>H<sub>29</sub>NO<sub>3</sub>S]<sup>-</sup>: 506.1729, found: 506.1729.

**L-2:** <sup>1</sup>H NMR (500 MHz, CDCl<sub>3</sub>) : δ(ppm) 7.84 (dd, *J* = 5.2, 3.4 Hz, 2H), 7.55 – 7.51 (m, 1H), 7.45 (dd, *J* = 10.4, 4.7 Hz, 2H), 7.12 (d, *J* = 6.3 Hz, 1H), 5.06 (dt, *J* = 7.7, 4.1 Hz, 1H), 4.29 (dd, *J* = 9.1, 7.1 Hz, 2H), 3.15 (ddd, *J* = 11.5, 9.0, 4.1 Hz, 2H), 1.41 (t, *J* = 9.0 Hz, 1H), 1.33 (t, *J* = 7.1 Hz, 3H); <sup>13</sup>C NMR (126 MHz, CDCl<sub>3</sub>): δ(ppm) 170.2, 167.0, 133.6, 132.0, 128.7, 127.2, 62.2, 54.0, 27.0, 14.2; HRMS(ESI<sup>+</sup>) [M+Na]<sup>+</sup>: calcd for C<sub>12</sub>H<sub>15</sub>NO<sub>3</sub>SNa 276.0665, found 276.0667.



Scheme S1 Syntheses of L/D-1.

### S1.3 REFERENCES

- (1) M. Baglan and S. Atlgan, *Chem Commun.*, 2013, **49**, 5325.
- (2) G. Liang, J. W. Y. Lam, W. Qin, J. Li, N. Xie and B. Z. Tang, *Chem Commun.*, 2014, **50**, 1725.

## S2. ADDITIONAL DATA

### S2.1 Spectral studies

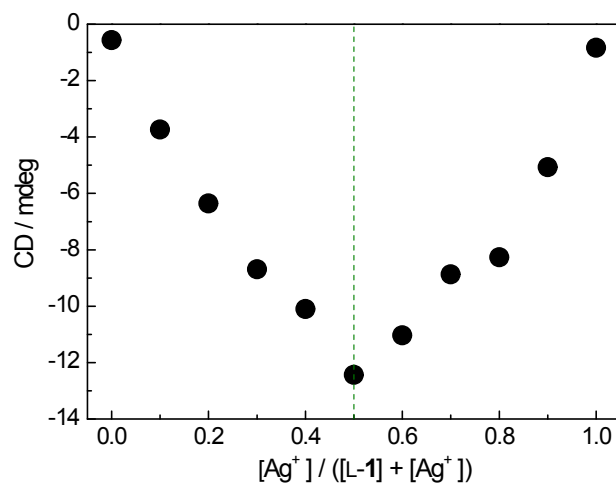


**Figure S1** Job plot for the interaction of  $\text{Ag}^+$  with L-1 in ethanol using CD signal at 290 nm. Total concentration of [L-1] and  $[\text{Ag}^+]$  was 20  $\mu\text{M}$ .

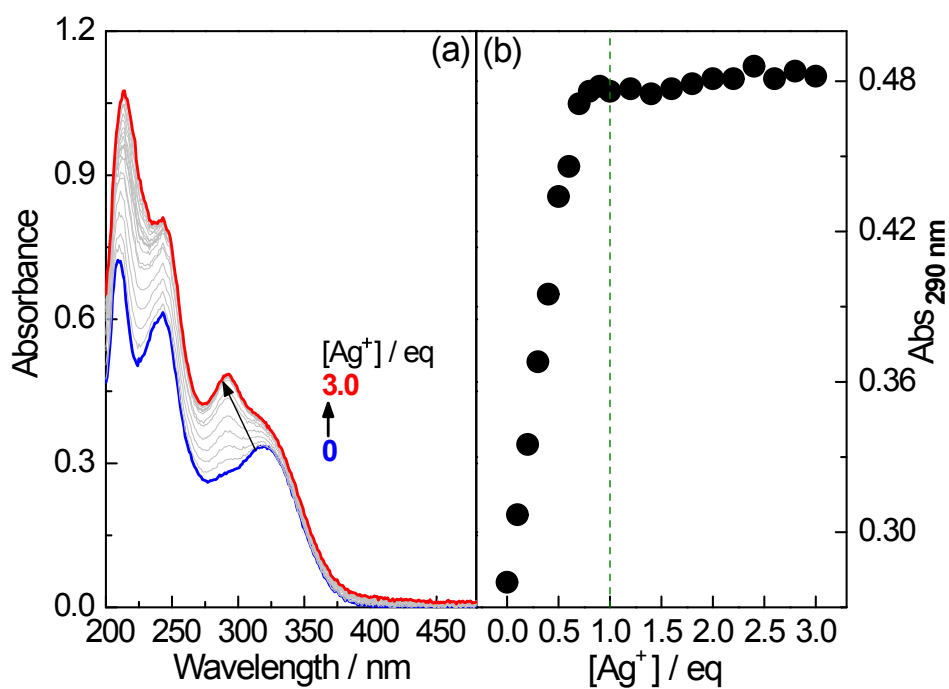


**Figure S2** (a) Absorption spectra of L-1 in EtOH in the presence of  $Ag^+$  and (b) plots of absorbance at 290 nm against concentration of  $[Ag^+]$ .  $[L-1] = 20 \mu M$ .

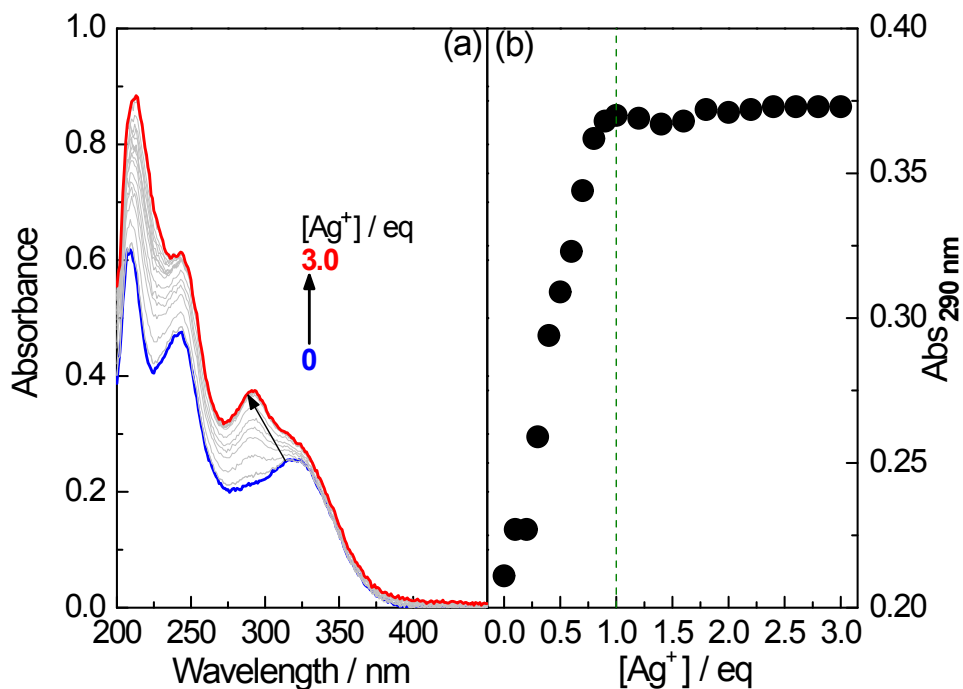


**Figure S3** (a) Absorption spectra of L-1 in EtOH in the presence of  $Ag^+$  and (b) plots of absorbance at 290 nm against concentration of  $[Ag^+]$ .  $[L-1] = 15 \mu M$ .

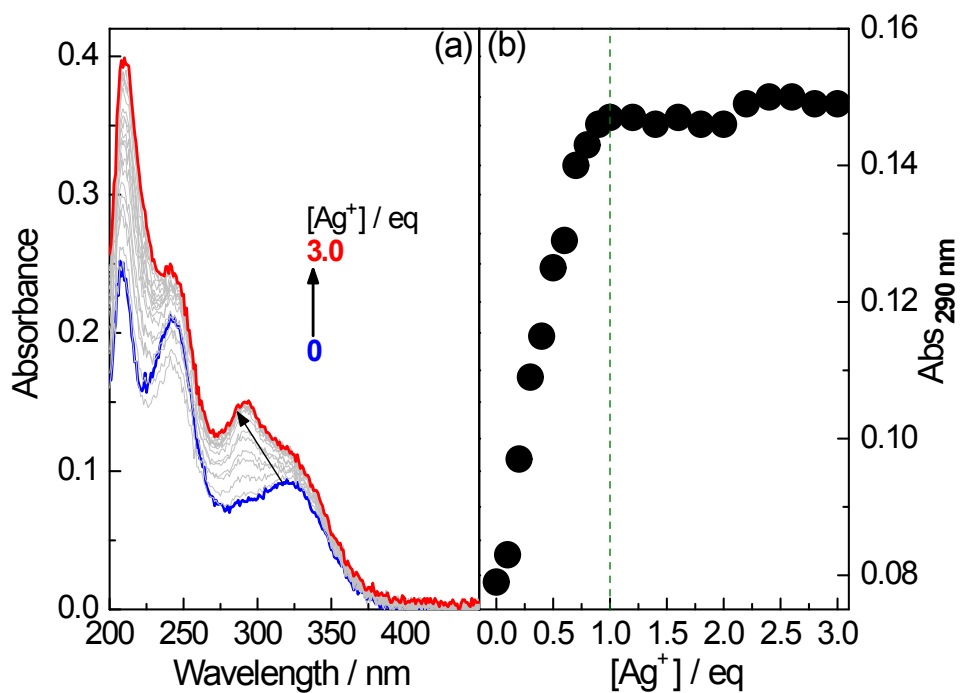


**Figure S4** (a) Absorption spectra of L-1 in EtOH in the presence of Ag<sup>+</sup> and (b) plots of absorbance at 290 nm against concentration of [Ag<sup>+</sup>]. [L-1] = 5 μM.

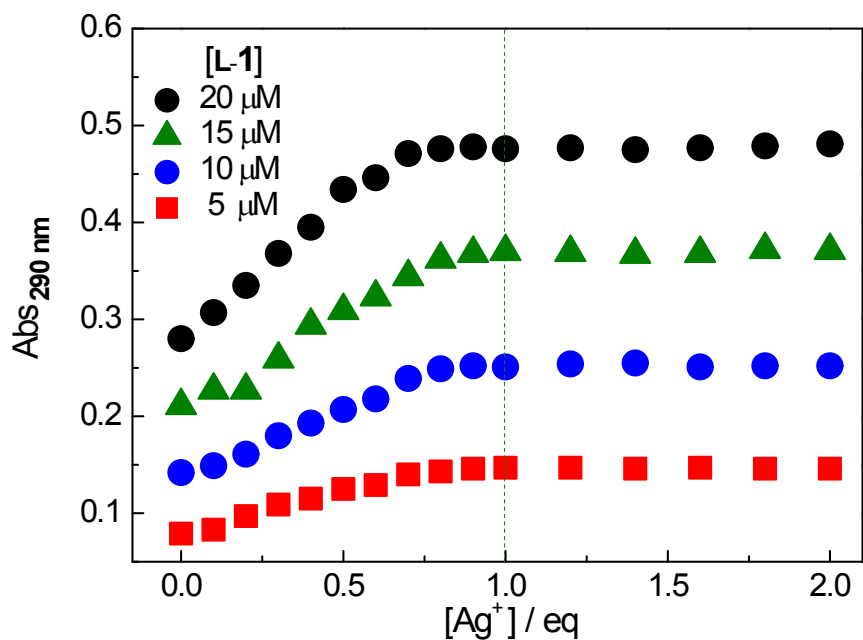


**Figure S5** Plots of absorbance at 290 nm of L-1 at varying concentration as a function of [Ag<sup>+</sup>].

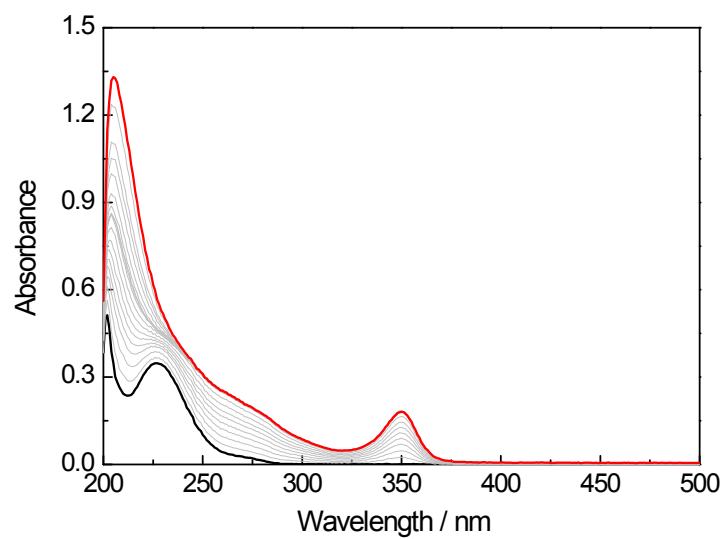


**Figure S6** Absorption spectra of L-2 in EtOH in the presence of Ag<sup>+</sup> of increasing concentration. [Ag<sup>+</sup>] = 0 - 75 μM and [L-2] = 25 μM.

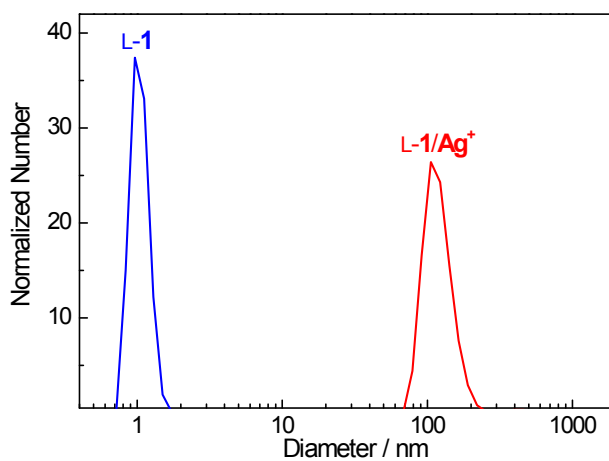


**Figure S7** Hydrodynamic diameters of L-1 in the absence or presence of Ag<sup>+</sup> in EtOH. [L-1] = [Ag<sup>+</sup>] = 5 μM.

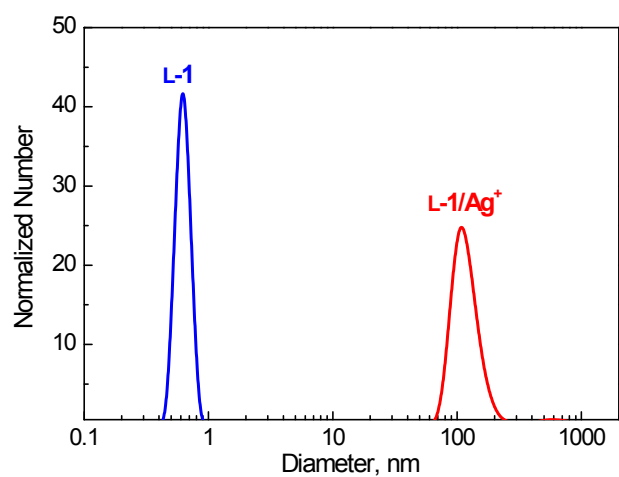


**Figure S8** Hydrodynamic diameters of L-1 in the absence or presence of  $\text{Ag}^+$  in EtOH.  $[\text{L-1}] = [\text{Ag}^+] = 10 \mu\text{M}$ .

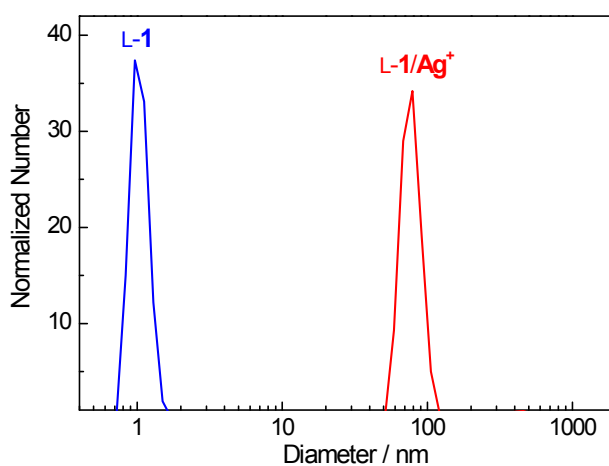


**Figure S9** Hydrodynamic diameters of L-1 in the absence or presence of  $\text{Ag}^+$  in EtOH.  $[\text{L-1}] = [\text{Ag}^+] = 15 \mu\text{M}$ .

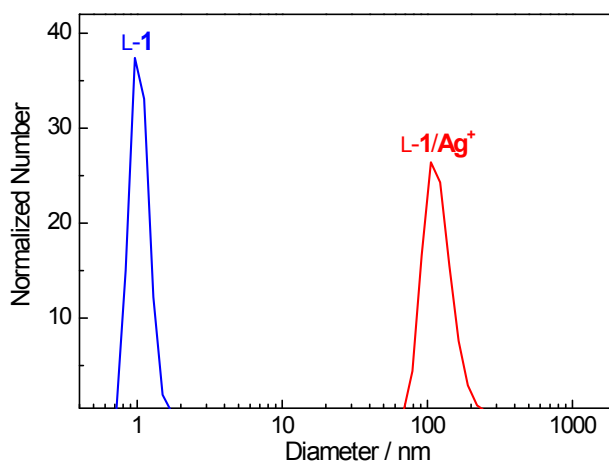




**Figure S10** Hydrodynamic diameters of L-1 in the absence or presence of  $\text{Ag}^+$  in EtOH.  $[\text{L-1}] = [\text{Ag}^+] = 20 \mu\text{M}$ .

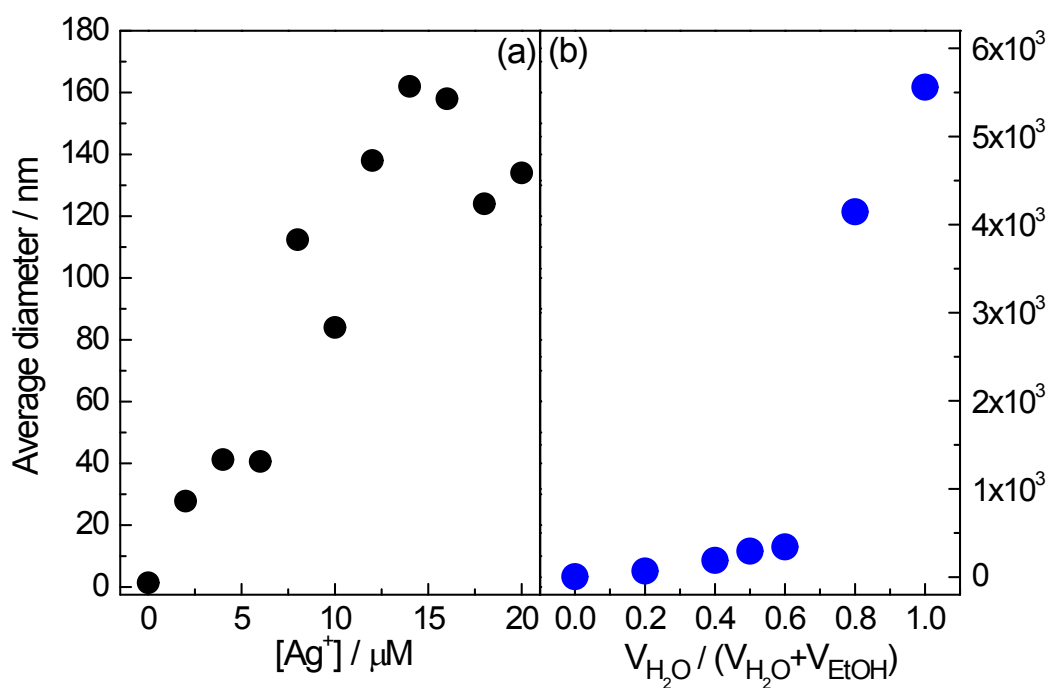


**Figure S11** Average hydrodynamic diameters of L-1 (a) in the presence of  $\text{Ag}^+$  in EtOH and (b) in EtOH containing increasing volume fraction of water.  $[\text{L-1}] = 20 \mu\text{M}$ .

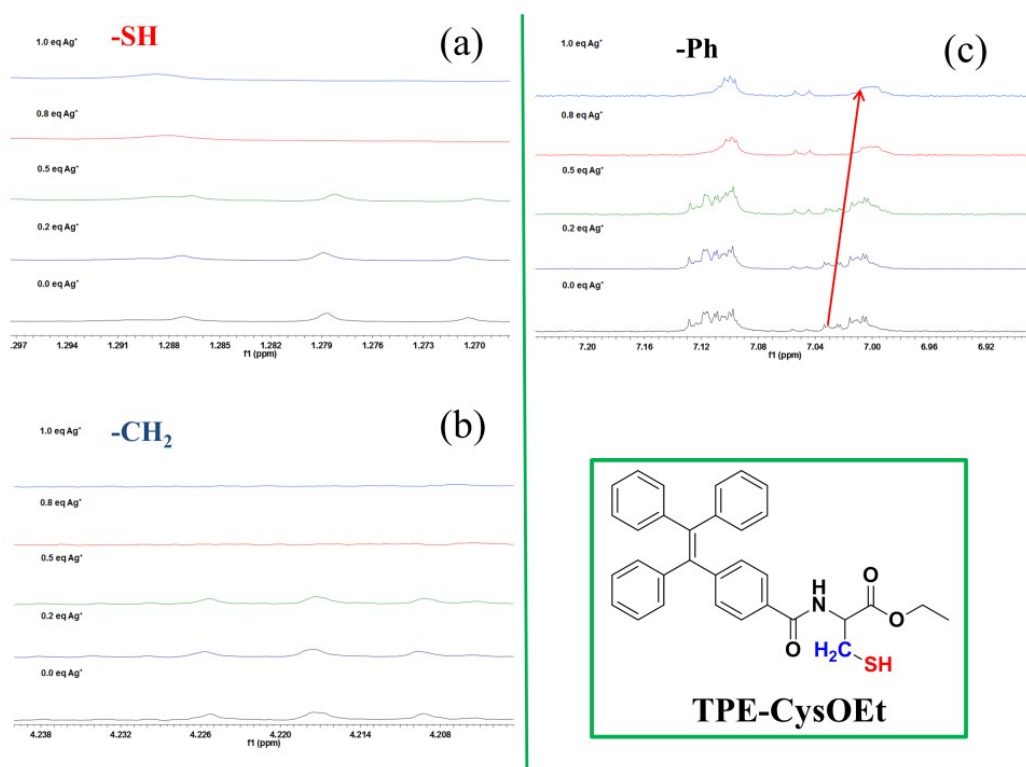


**Figure S12** Traces of  $^1\text{H}$  NMR titration of L-1 by  $\text{Ag}^+$  in  $\text{CD}_3\text{OD}$  in the regions of resonance of -

SH (a), -CH<sub>2</sub> (b) and -phenyl (c). The fact that the signals of the aromatic protons become well-resolved upon titration (c) indicates the formation of ordered structures. [L-1] = 100 μM.

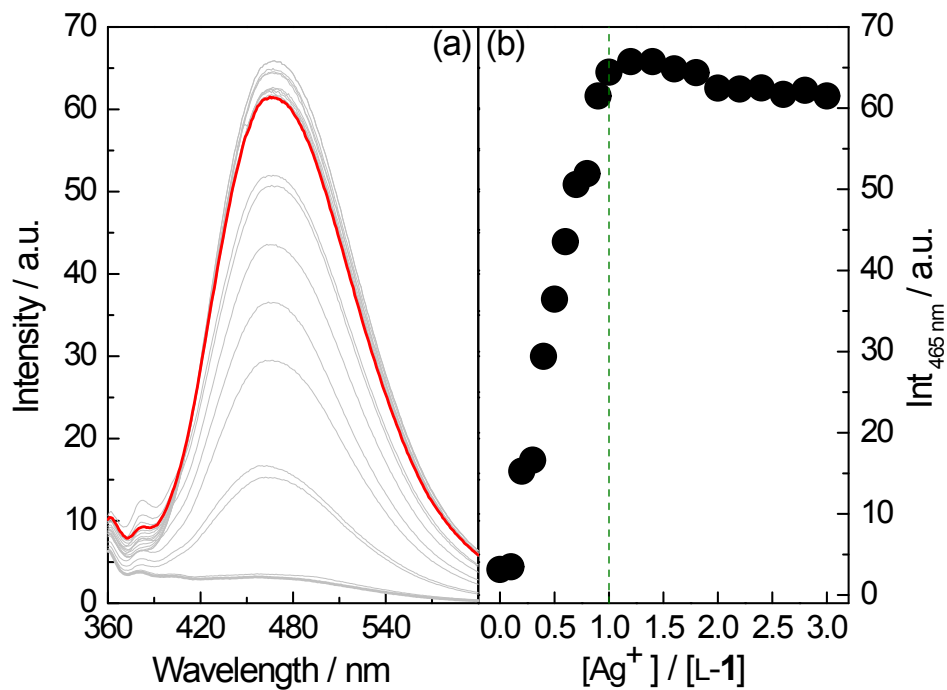


**Figure S13** Fluorescence spectra of L-1 in EtOH in the presence of Ag<sup>+</sup> (a) and plot of fluorescence intensity at 465 nm against [Ag<sup>+</sup>] (b). [L-1] = 20 μM, [Ag<sup>+</sup>] = 0 - 60 μM. λ<sub>ex</sub> = 325 nm.

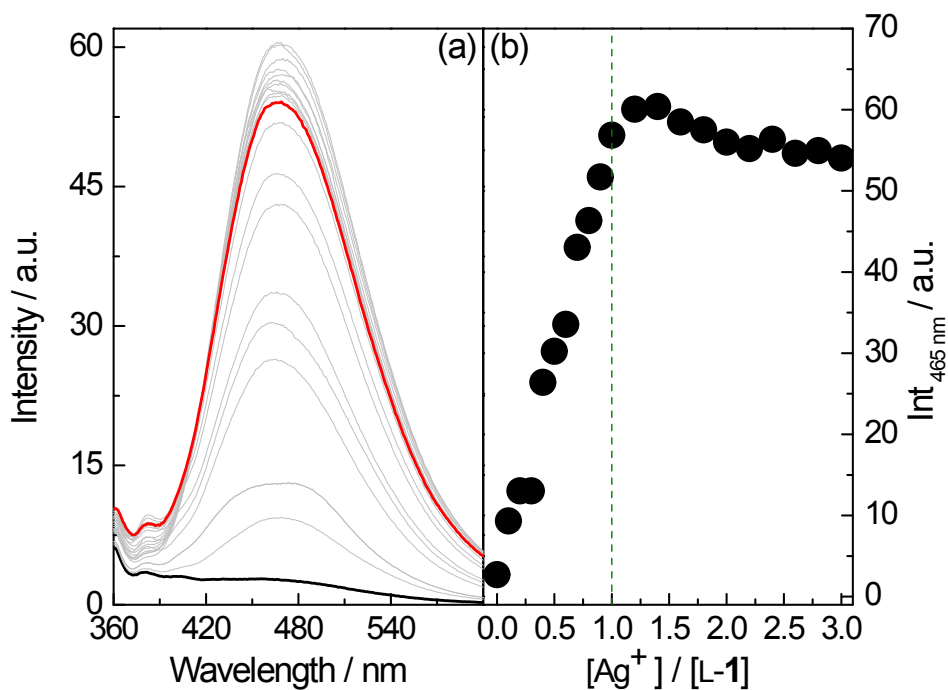


**Figure S14** Fluorescence spectra of L-1 in EtOH in the presence of  $\text{Ag}^+$  (a) and plot of intensity at 465 nm against  $[\text{Ag}^+]$  (b).  $[\text{L-1}] = 15 \mu\text{M}$ ,  $[\text{Ag}^+] = 0 - 45 \mu\text{M}$ .  $\lambda_{\text{ex}} = 325 \text{ nm}$ .

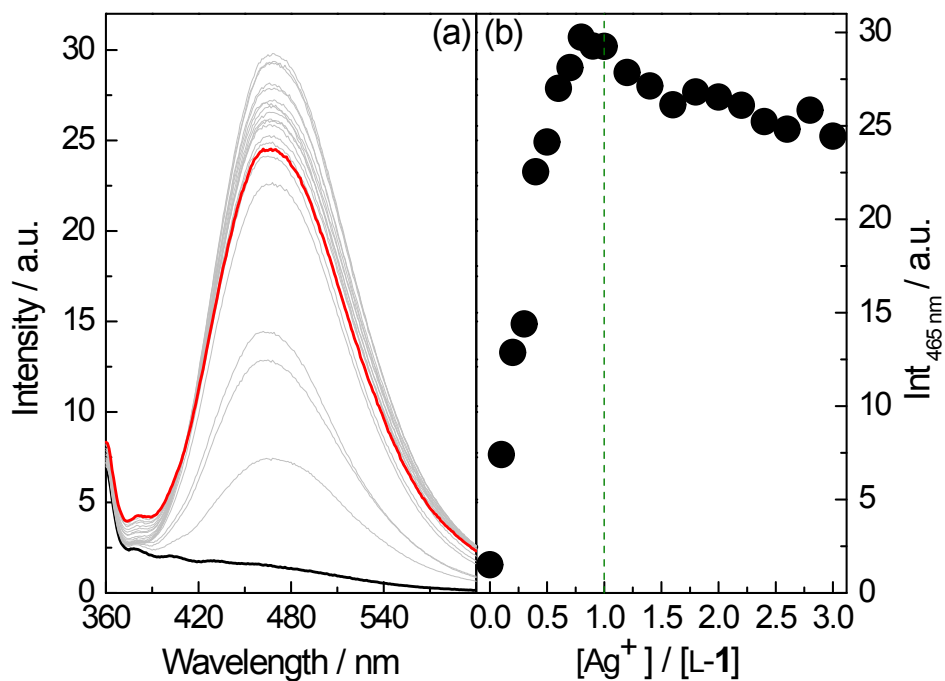


**Figure S15** Fluorescence spectra of L-1 in EtOH in the presence of  $\text{Ag}^+$  (a) and plot of intensity at 465 nm against  $[\text{Ag}^+]$  (b).  $[\text{L-1}] = 5 \mu\text{M}$ ,  $[\text{Ag}^+] = 0 - 15 \mu\text{M}$ .  $\lambda_{\text{Ex}} = 325 \text{ nm}$ .

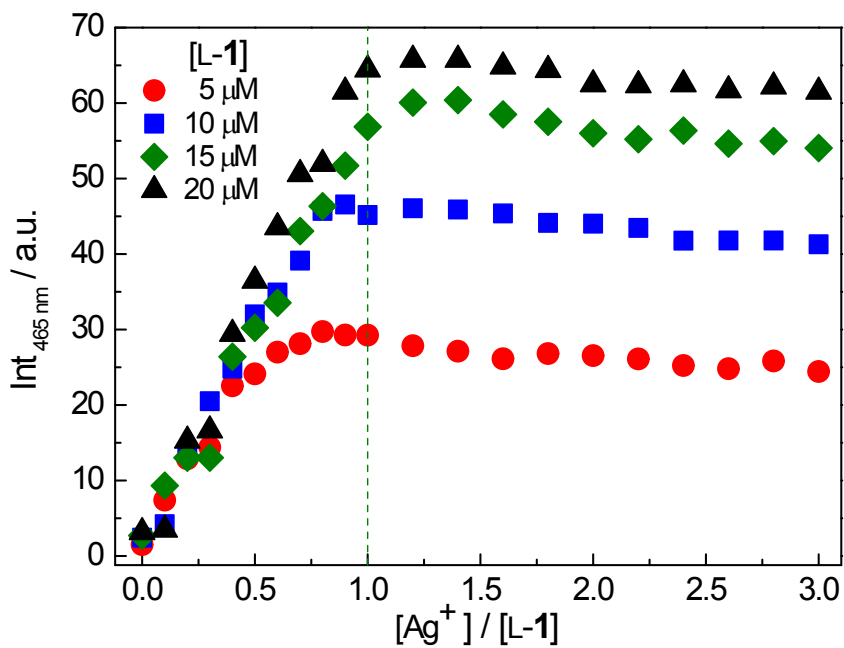


**Figure S16** Plots of fluorescence intensity at 465 nm of L-1 at different concentration in EtOH versus concentration of  $\text{Ag}^+$ .

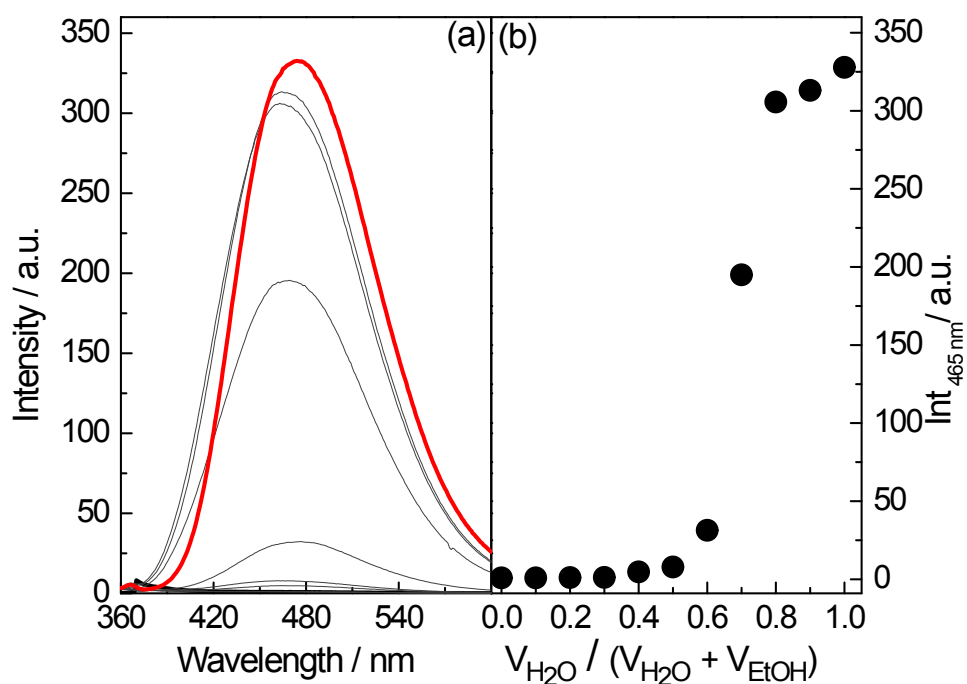


**Figure S17** (a) Fluorescence spectra of L-1 in binary solvents of EtOH and H<sub>2</sub>O of different composition and (b) plots of fluorescence intensity at 465 nm against water volume fraction. [L-1] = 10 μM, V<sub>H<sub>2</sub>O</sub> + V<sub>EtOH</sub> = 2 mL; λ<sub>Ex</sub> = 325 nm.

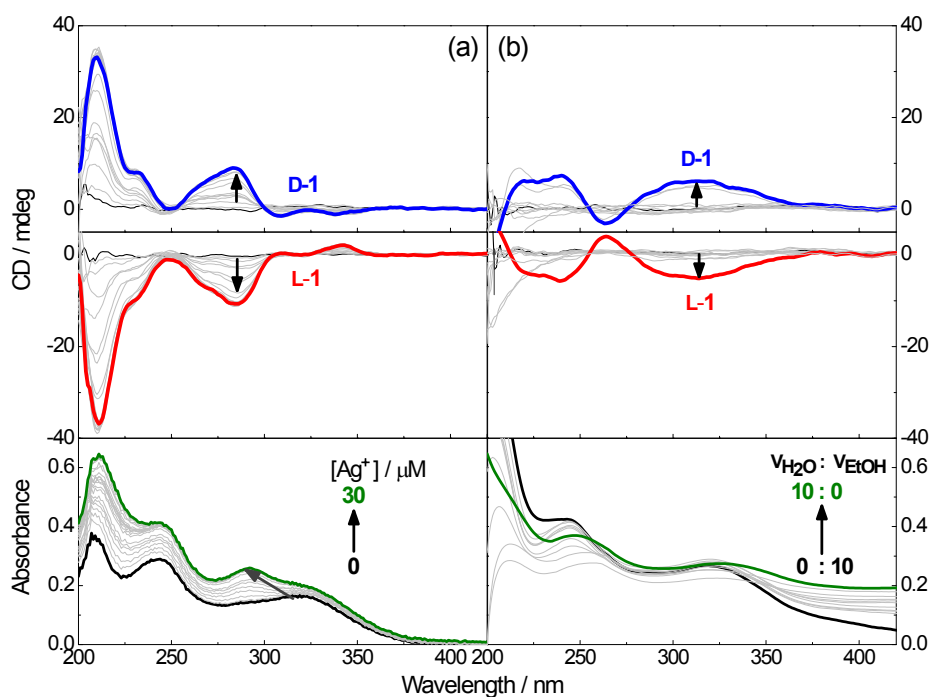


**Figure S18** Absorption and CD spectra of D/L-1 in EtOH (a) in the presence of Ag<sup>+</sup> and (b) with

increasing H<sub>2</sub>O volume fraction. [1] = 10 μM, [Ag<sup>+</sup>] = 10 μM.

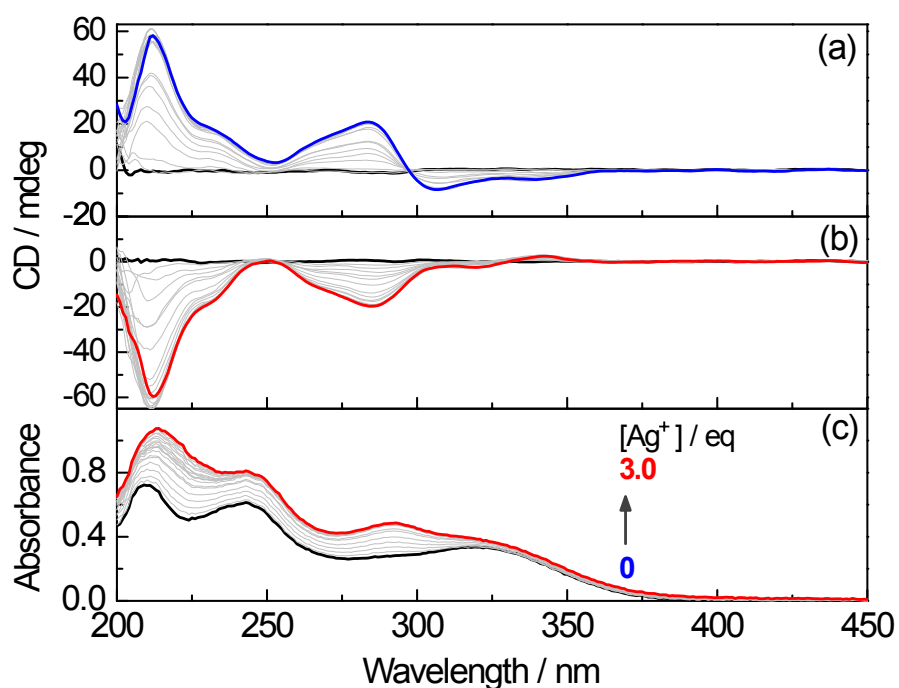


**Figure S19** Absorption (c, L-) and CD (a, D-; b, L-) spectra of **1** in EtOH in the presence of Ag<sup>+</sup> of increasing concentration. [1] = 20 μM.

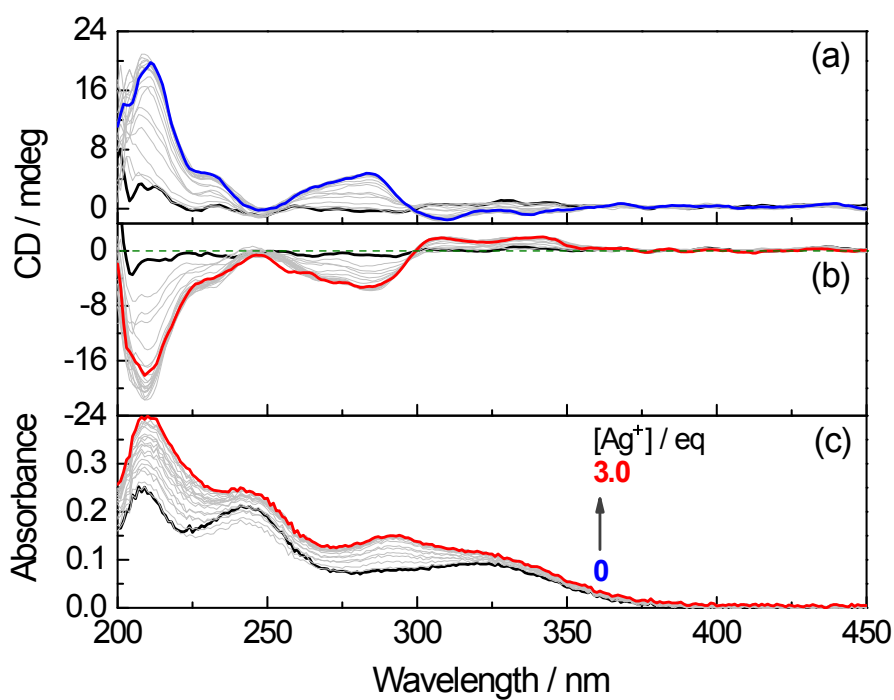


**Figure S20** Absorption (c, L-) and CD (a, D-; b, L-) spectra of **1** in EtOH in the presence of Ag<sup>+</sup> of increasing concentration. [1] = 5 μM.

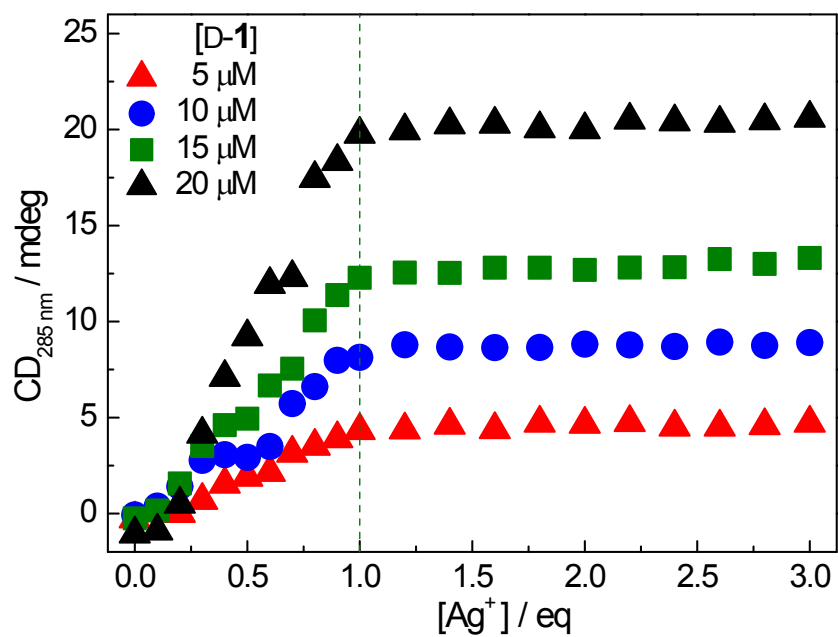


**Figure S21** Plots of CD signal at 285 nm of D-1 at different concentration as a function of Ag<sup>+</sup> in EtOH.

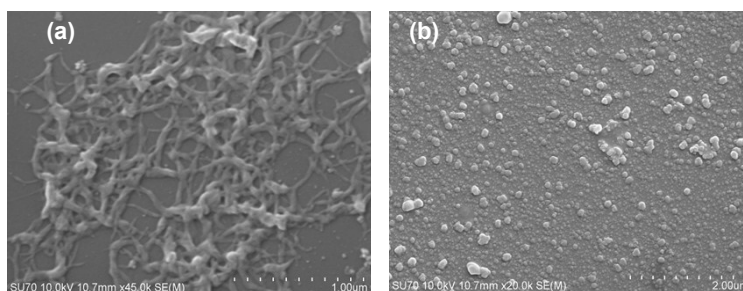


**Figure S22** SEMs of the coordination polymers of L-1-Ag<sup>+</sup> in EtOH (a) and aggregates of L-1 in water (b). [1] = 10 μM, [Ag<sup>+</sup>] = 10 μM.

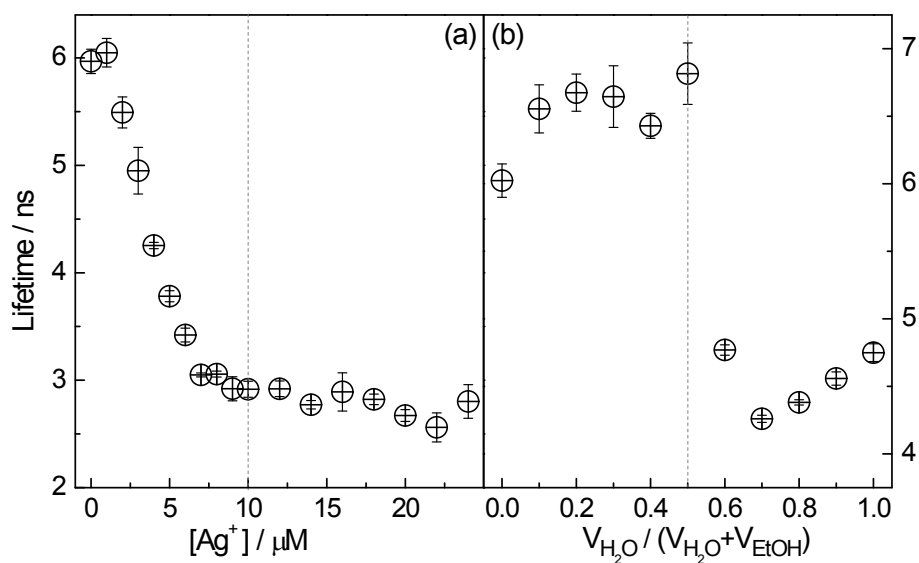


**Figure S23** Fluorescence lifetime of L-1 in EtOH as a function of the concentration of Ag<sup>+</sup> (a) and volume fraction of water (b). [L-1] = 10 μM; λ<sub>Ex</sub> = 339 nm, λ<sub>Em</sub> = 465 nm.

**Table S1** Quantum yields of L-1 in EtOH containing increasing volume fraction of water <sup>a</sup>

V <sub>H<sub>2</sub>O</sub> /(V <sub>H<sub>2</sub>O</sub> +V <sub>EtOH</sub> )	0	0.2	0.4	0.5	0.6	0.8	1.0
Φ / %	0.01	0.03	0.12	0.15	20.6	32.16	52.42

<sup>a</sup> [L-1] = 10 μM; λ<sub>Ex</sub> = 325 nm, λ<sub>Em</sub> = 465 nm.

**Table S2** Quantum yields of L-1 in EtOH containing Ag<sup>+</sup> of different concentration <sup>a</sup>

[Ag <sup>+</sup> ] / μM	0	2	4	6	8	10	12	14	16	18	20	22	24
Φ / %	0.01	0.04	0.35	0.58	0.74	1.84	1.53	1.45	1.22	1.17	1.13	1.12	1.11

<sup>a</sup> [L-1] = 10 μM; λ<sub>Ex</sub> = 325 nm, λ<sub>Em</sub> = 465 nm.

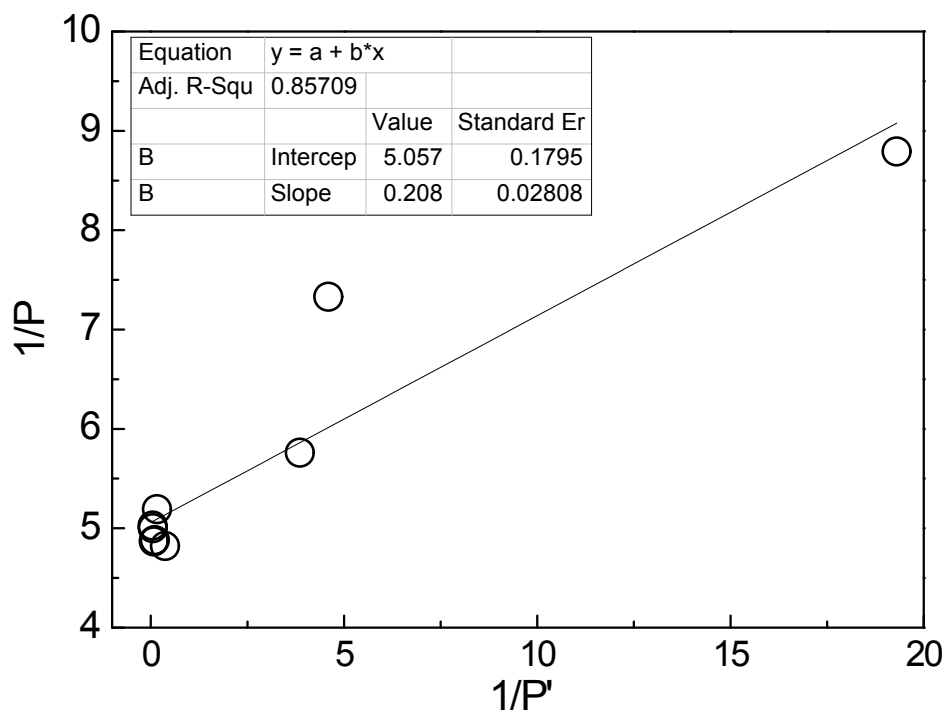


**Figure S24** Plots of reciprocal polarization ( $1/P$ ) of L-1 in EtOH in the presence of 0 - 2 eq  $Ag^+$  versus calculated parameter  $1/P'$ .  $P$  is the measured polarization.  $1/P'$  was calculated from  $RT\tau/\eta V$  defined in Perrin equation, in which  $R$  is gas constant,  $T$  is absolute temperature,  $\tau$  is lifetime,  $\eta$  is solution viscosity, and  $V$  is volume calculated by the diameter data from DLS measurements. [L-1] = 10  $\mu M$ ;  $\lambda_{Ex}$  = 325 nm,  $\lambda_{Em}$  = 465 nm.

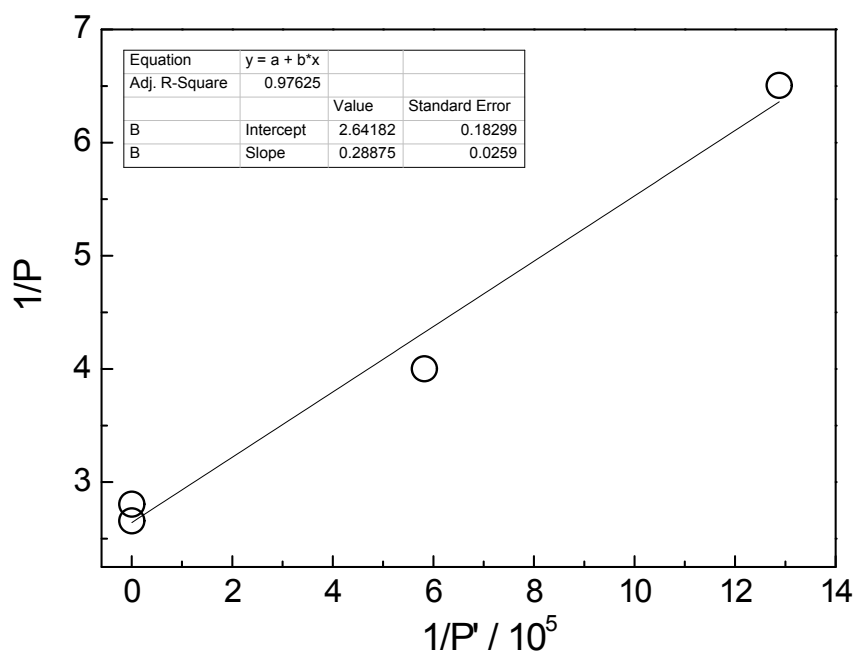




**Figure S25** Plots of reciprocal of polarization ( $1/P$ ) of L-1 in EtOH-H<sub>2</sub>O mixtures of varying water volume fraction against  $1/P'$ .  $P$  is the measured polarization.  $1/P'$  was calculated from  $RT\tau/\eta V$  defined in Perrin equation, in which  $R$  is gas constant,  $T$  is absolute temperature,  $\tau$  is lifetime,  $\eta$  is solution viscosity, and  $V$  is volume calculated by the diameter data from DLS measurements.  $\lambda_{\text{Ex}} = 325 \text{ nm}$ ,  $\lambda_{\text{Em}} = 465 \text{ nm}$ .

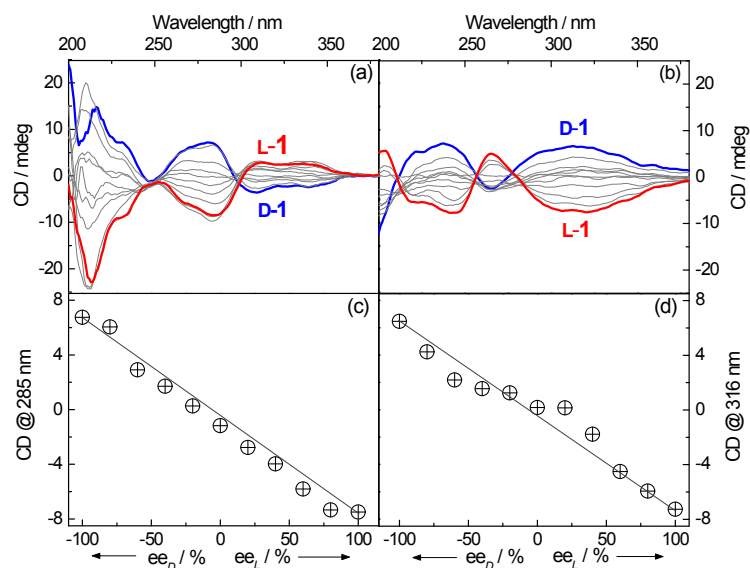


**Figure S26** CD spectra and plots of CD signal of **1** against  $ee$  in ethanol in the presence of 1 eq  $\text{Ag}^+$  (a, and b for CD signal at 285 nm) and in 9:1 (v/v) H<sub>2</sub>O-EtOH (c, and d for CD signal at 316 nm).  $[\text{L-1}] + [\text{D-1}] = 10 \mu\text{M}$ ,  $[\text{Ag}^+] = 10 \mu\text{M}$ .

## S2.1 <sup>1</sup>H and <sup>13</sup>C NMR spectra of L- and D-1

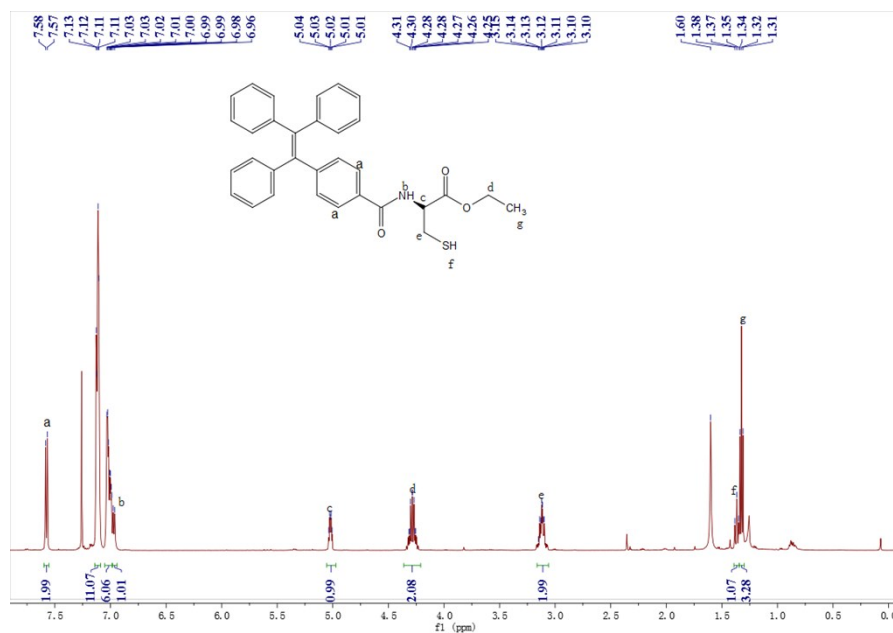


Figure S25 <sup>1</sup>H NMR of D-1 (500 MHz, CDCl<sub>3</sub>)

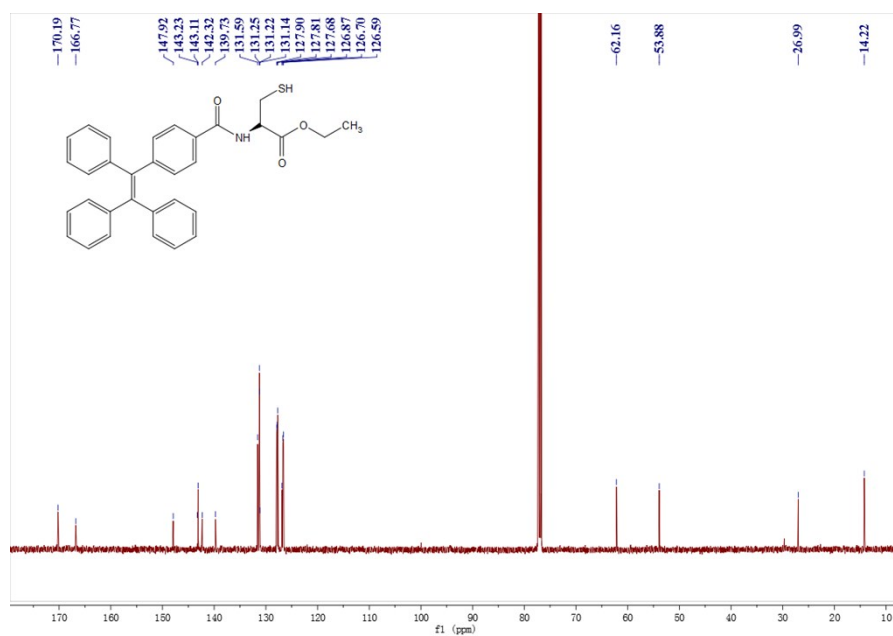


Figure S26 <sup>13</sup>C NMR of D-1 (126MHz, CDCl<sub>3</sub>)

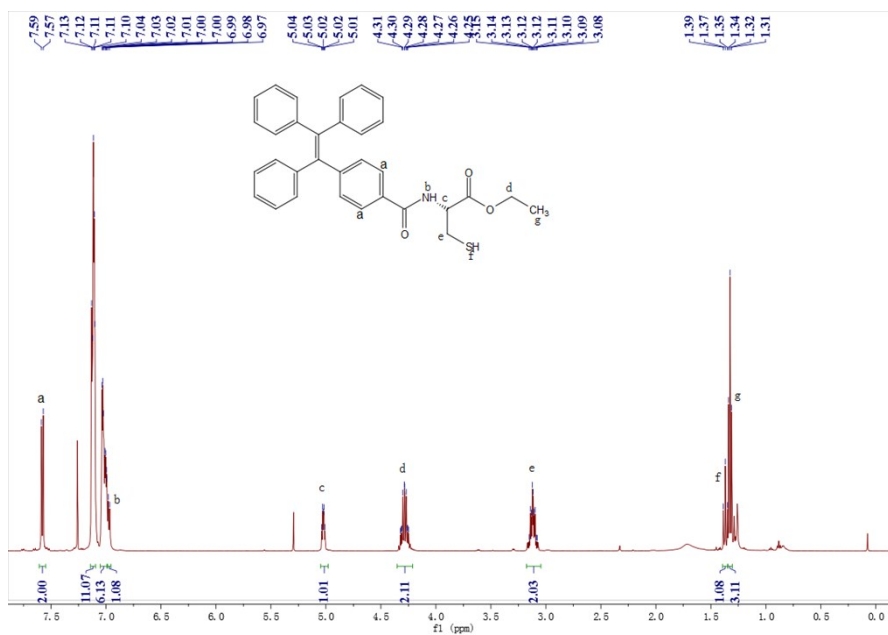


Figure S27 <sup>1</sup>H NMR of L-1 (500 MHz, CDCl<sub>3</sub>)

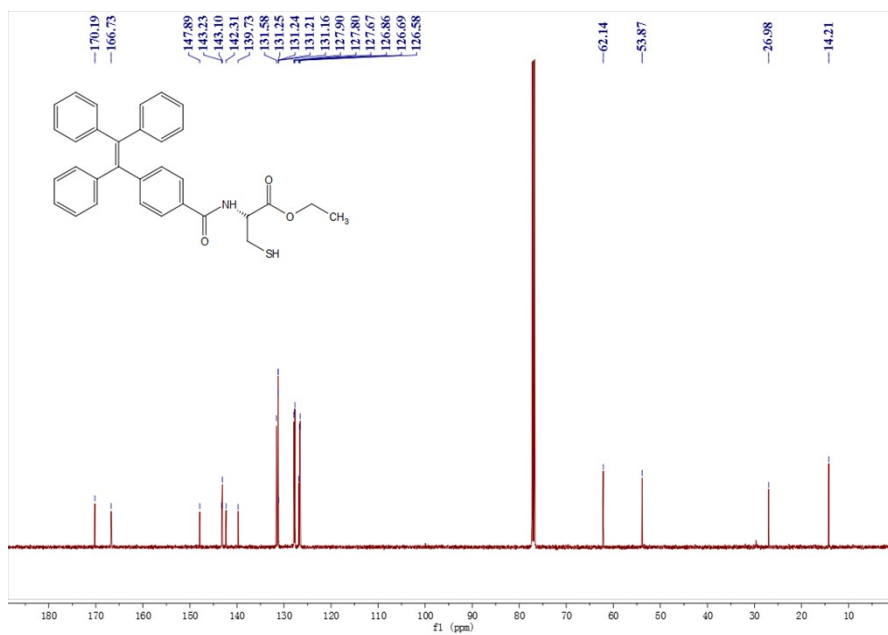


Figure S28 <sup>13</sup>C NMR of L-1 (126 MHz, CDCl<sub>3</sub>)

